Wear 311 (2014) 123–129

Contents lists available at ScienceDirect

Wear

journal homepage: www.elsevier.com/locate/wear

The segmentation of wear particles in ferrograph images based on an improved ant colony algorithm

Jingqiu Wang [a,*], Long Zhang [a], Fengxia Lu [a,b], Xiaolei Wang [a,b]

[a] College of Mechanical and Electrical Engineering, Nanjing University of Aeronautics and Astronautics, Nanjing 210016, China
[b] Jiangsu Key Laboratory of Precision and Micro-Manufacturing Technology, Nanjing 210016, China

ARTICLE INFO

Article history:
Received 8 October 2013
Received in revised form
8 January 2014
Accepted 10 January 2014
Available online 21 January 2014

Keywords:
Ferrography
Wear
Wear particle segmentation
Ant colony clustering

ABSTRACT

Ferrography is a notably useful means to determine the wear condition of machines. Before attempting to extract the feature parameters of wear particles for identification and analysis, it is necessary to separate wear particles in ferrograph images. Hence, wear particle segmentation is a critical first step for intelligent ferrography based on computer image analysis. This paper presents a new method for the segmentation of wear particles by combining watershed and an improved ant colony clustering algorithm. The experimental results have demonstrated the possibility of achieving accurate segmentation of wear particles, including large abnormal wear particles and deposited chains.

1. Introduction

Ferrography was developed in the 1970s as a technology for monitoring wear condition and diagnosing failure. Ferrography determines the wear status and wear mechanisms of equipment through quantitative and qualitative analysis of the quantity, size, shape, color and surface texture of wear particles in a lubrication system. Ferrography is particularly efficient for examining large particles, which is extremely important for monitoring the conditions of, for instance, jet engines [1], transmissions [2,3] and mining equipment.

The problem with currently employed ferrography techniques is that the particle morphology assessment, particle classification and the machine status evaluation rely on human expertise, which is time-consuming, costly and not always reliable [4]. During the last three decades, considerable efforts have been made in the application of image processing techniques for feature extraction and wear particle recognition to improve the efficiency and accuracy of ferrography analysis [5–12]. Analysis systems based on human-computer interaction, such as the CAVE, CASPA, SYCLOPS [13], as well as expert systems based on 3D particle-analysis [14] and automatic particle-identification systems [15], have been developed.

However, because the wear particles are deposited onto the glass substrate by a magnetic field, the ferro-particles often deposit in the form of chains, which may be composed of a number of fine abrasive particles or may contain a number of large abnormal wear particles, which are generated from abnormal wear, usually larger than 15 μm. As shown in Fig. 1, the particles may be connected and even overlapped, depending on the concentration. In addition, the random, complex morphology (shape, color, surface texture), and blur edges of wear particles may also lead to difficulties in computer-aided ferrography analysis.

Before attempting to extract feature parameters of wear particle for morphology analysis and identification, it is necessary to separate wear particles from each other, i.e., wear particle segmentation. The accuracy of segmentation will directly affect the subsequent feature extraction, classification and identification of wear particles. Therefore, wear particle segmentation is the critical first step for intelligent ferrography based on computer image analysis. Because of this step's importance, more attention should be paid to separate wear particles in chains, as the segmentation of wear particles is even more difficult than the recognition of the particles [16].

For the segmentation of a ferrograph image, to the best of our knowledge, existing studies are largely concentrating on the segmentation of wear particles from the background of the image [17,18].

Ferrograph images are obtained using an optical microscope with transmitted and reflected lights. Different combinations of transmitted and reflected light will result in different background colors in the images. Hence, it is not easy to separate wear particles and background based on the traditional gray histogram threshold method, because no matter where the threshold is set, a

* Corresponding author.
E-mail address: meejqwang@nuaa.edu.cn (J. Wang).

0043-1648/$ - see front matter © 2014 Elsevier B.V. All rights reserved.
http://dx.doi.org/10.1016/j.wear.2014.01.004

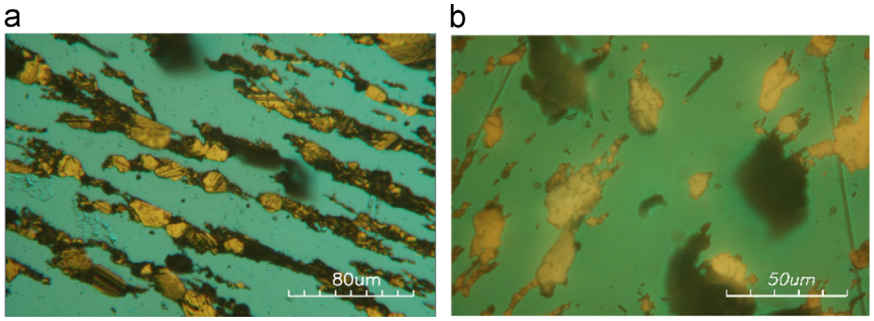

Fig. 1. Typical ferrograph images. (a) Wear particle chains, and (b) large abnormal wear particles with blurred edges.

number of overly bright or overly dark wear particles may be mistaken as image background and thereby result in incomplete segmentation.

It has been demonstrated that accurate segmentation could be obtained using the threshold method in color space, rather than in gray space [17]. Furthermore, color information can be used along with in-depth applications of image processing techniques in wear particle analysis to determine the wear modes and material of wear particles. Chen et al. indicated that the RGB or HSV color space should be used in the segmentation between wear particles from image background, while fuzzy clustering techniques could be used for the segmentation [18]. In our previous research, we compared the segmentation and clustering effects for ferrograph images in different color space, and proposed a 2D k-means color-clustering algorithm in CIELAB color space which used two color components (a, b) for segmentation, and omitted the luminance component to reduce the adverse effects of brightness for image segmentation [19].

The segmentation of wear particles from particle chains has also been challenged by many researchers. Li et al. used morphological erosion and dilation operations on binary images, the edge of a single wear particle could be detected with the Laplace operation [20]. Hu et al. applied pretreatment techniques, including image enhancement, image segmentation, filling pore and image erosion, to ferrograph images. Subsequently, high-brightness wear particles were extracted from deposited chains using the adaptive threshold method [21].

However, the existing segmentation methods are not adaptable for complicated ferrograph images, there remains a large gap in the applications.

How to segment the wear particles effectively, particularly the large abnormal particles within the deposited chains, and to facilitate the further identification of wear particles is the key issue facing current ferrograph image analysis.

This research attempts to solve the abovementioned difficult problems, i.e., the segmentation and clustering of the wear particles on ferrograph images, to improve the level of intelligent and automatic analysis for ferrograph images. Therefore, we propose two new segmentation methods for ferrograph images. First, an improved ant colony optimization is applied to extract edges of wear particles. Second, a hybrid method based on marker-watershed and ant colony clustering algorithm is proposed to obtain the accurate segmentation of wear particles, especially the large abnormal wear particles. The segmentation methods are subsequently evaluated using real ferrograph images.

2. Principle of ant colony optimization

Normally, most of image segmentation approaches are based on two strategies, e.g., recognizing contour or generating regions in view of homogeneity. Traditional techniques, such as threshold method, template matching, region growing and feature clustering, have been demonstrated to be successful in many applications. Artificial intelligences, such as neural networks and genetic algorithms in image analysis, could be considered to be alternate approaches, but none of them is generally applicable to all images and different algorithms are not equally suitable for a particular application [22].

The first ant algorithm, named “Ant System”, was proposed in the 1990s by Dorigo et al. [23]. This algorithm was followed by the development of a number of ant colony optimization (ACO) algorithms [24].

ACO is a population-based meta-heuristic algorithm motivated by the food foraging behavior of real ant colonies. While foraging, real ants deposit pheromones on the ground to mark favorable paths that should be followed by other members of the colony. Greater quantities of pheromones on the path mean that there is a higher probability of finding food. However, as the pheromones evaporate, this condition leads to the disappearance of certain paths if no ants follow these paths. Therefore, in the end, only better and shorter paths remain.

In an artificial or computer environment, ACO has two major steps, e.g., path construction and pheromone update.

In the step of path construction, each ant selects a next suitable path and moves from one node to another according to a transition probability function. The transition probability between node i to j is determined as follows [23]:

$$p_{ij}=\begin{cases}\dfrac{\tau_{ij}^{\alpha}(t)\eta_{ij}^{\beta}(t)}{\sum_{s\in S}\tau_{is}^{\alpha}(t)\eta_{is}^{\beta}(t)}, & j\in S,\\ 0, & \text{otherwise}\end{cases}, \tag{1}$$

where S is the set of all available paths that an ant can choose in one step, α and β are adjustment factors for preventing all ants moving along the same path to obtain the same results, $\eta_{ij}(t)$ stands for the heuristic guide function, and $\tau_{ij}(t)$ represents the pheromone concentration on the path p_{ij} at moment t.

In the pheromone update step, the pheromone concentration on each path is updated according to the following formula:

$$\tau_{ij}(t')=(1-\rho)\tau_{ij}(t)+\Delta\tau_{ij}, \tag{2}$$

where ρ is the pheromone evaporate constant, such that if no ants pass through a path after a certain time, the pheromone on that path gradually evaporates, $\Delta\tau_{ij}$ is the increase of pheromone concentration on the path after one cycle:

$$\Delta\tau_{ij}=\sum_{k=1}^{N}\Delta\tau_{ij}^{k}, \tag{3}$$

where N is the number of ants and $\Delta\tau_{ij}^{k}$ is the pheromone concentration left on the path by the kth ant.

Pheromone updating leads ants to search for better solutions for successive iterations. After the algorithm reaches the termination condition (which can be the maximum number of

iterations or time), the best-so-far ant path is selected as a solution to the algorithm.

Due to such attractive features as being discrete, parallel and robust, the ACO algorithm can be adopted for image processing and object detection. For example, ant-inspired algorithms were developed for image edge extraction [25–29], and they were also used as intelligent clustering methods for image segmentation [30–34].

In most of the abovementioned studies, heuristic information for the movement of ants is decided by values of pixels in the gray level gradient. Only paper [33,34] worked on the solution of segmentation and object detection in color images, whereby the experimented results are presented on natural images, medical images and remote sensing images.

Inspired by the above survey, we seek a segmentation method based on the ant colony algorithm as the solution to the segmentation of wear particles in color ferrograph images.

3. Edge detection of wear particles based on improved ant colony optimization (IACO)

Wear particle edges usually refer to the set of pixels at which image brightness changes sharply. Wear particle edges exist between wear particles and image background or between wear particles. Various parameters representing shape characteristics or outline profiles of wear particles can be extracted from the edges of wear particles. Moreover, the edge is an important feature that can be exploited effectively to identify particles in relation to the ongoing wear processes.

The main principle of wear particle edge detection based on IACO is the following.

The pixels in the image to be processed can be considered as the nodes of a graph in which ants move from one pixel to another following the transition probabilities. The transition probability depends on the heuristic information and pheromone concentration. The heuristics information for edge detection is determined by local statistics (e.g., gradient) of the pixel. An ant will deposit a certain amount of pheromones when it visits a pixel. The more ants visit a pixel, the more pheromone deposition will be on that pixel. In the end, edges can be detected by analyzing the pheromone distribution in the image.

The detailed steps of IACO are as follows.

3.1. Pretreatment of color ferrograph image

Conventional edge extraction method is often performed on gray-scale images. As mentioned above, the use of the color information can obtain better edge detection results. In this algorithm, a color image is decomposed to R, G and B three-component images. The morphological gradients of each component image are then calculated as G_i (x, y), $i=1,2,3$, respectively. Thus, the morphological gradient image G_{color} (x, y) is defined as

$$G_{color}(x,y)=\sum q_i G_i(x,y) \quad i=1,2,3, \tag{4}$$

where q_i is the weighting factor. In this algorithm, $q_i=1/3$, $i=1$, 2, 3.

The morphological opening and closing reconstruction operation are used on the morphological gradient image to eliminate noise. Fig. 2(a) is an original image, and Fig. 2(b) is the reconstructed gradient image.

3.2. The preliminary extraction of wear particle edges

To extract edges of wear particles, first, the traditional threshold algorithm is applied to the morphological gradient image. The result is shown in Fig. 2(c). It is noted that a large number of points lie on or close to the edges, and accordingly, these points are called initial edge points. The improved ACO is later applied to these initial points to obtain the accurate edges of wear particles.

3.3. IACO for the edge detection of wear particles

The IACO algorithm for edge detection of wear particles is an iterative process that includes the following steps:

(1) Ant distribution.
At the initial time of each cycle, a certain number of ants are randomly distributed on the initial edge points, and they later search the neighboring points in accordance with certain rules. Because ant searching is a time-consuming process, it is important to select the appropriate number of ants. For an $M\times N$ size of ferrograph image, the total number of ants is $\sqrt{M\times N}$.

(2) Ant searching rule.
Each artificial ant has its own memory. A Tabu list is used to describe ant memory. Tabu_k is the list of pixels that the kth ant has already visited. The Tabu list effectively avoids becoming stuck in a forward-backward loop.
If an ant finds itself surrounded by the pixels that are either in the Tabu list or occupied by other ants, it is randomly displaced to another unoccupied pixel that is not in the Tabu list. Otherwise, the ant moves from the current pixel (r, s) to one of its 8-neighboring pixels (i, j), according to the maximum probability searching rule (transition probability) [27]

$$p^k_{(r,s),(i,j)}=\begin{cases}\dfrac{\tau^{\alpha}_{(i,j)}(t)\eta^{\beta}_{(i,j)}(t)}{\sum_u\sum_v \tau^{\alpha}_{(u,v)}(t)\eta^{\beta}_{(u,v)}(t)}, & (i,j) \text{ and } (u,v)\notin \text{tabu}^k,\\ 0, & \text{otherwise},\end{cases} \tag{5}$$

where $\tau_{(i,j)}(t)$ is the pheromone concentration and $\eta_{(i,j)}(t)$ is the heuristic information of pixel (i, j).
Normally, the heuristic function is defined as

$$\eta_{(i,j)}(t)=\frac{G_{(i,j)}(x,y)}{C}, \tag{6}$$

where $G_{(i,j)}(x,y)$ denotes the gradient of pixel (i, j) and C is a constant that usually takes $C=256$.
In this study, not only is the gradient but also the color difference between two pixels is considered. Thus, the improved heuristic function is defined as

$$\eta^*_{(i,j)}(t)=\frac{G_{(i,j)}(x,y)}{\Delta a_{(r,s)(i,j)}+\Delta b_{(r,s)(i,j)}+c}, \tag{7}$$

where Δa and Δb denote the absolute difference of component a and b in the CIELAB color space between pixel (r, s) and (i, j), respectively, and c is the adjustment factor that serves to prevent Δa and Δb from being zero simultaneously, which would lead to the denominator of the heuristic function being zero when usually, $c=1$.
As the memory of an ant is limited, the Tabu list is updated after each ant selects a new pixel.

(3) Pheromone updating rule.
After all ants have moved once, the pheromone level of each pixel is updated according to the following formula:

$$\tau_{(i,j)}(t')=(1-\rho)\tau_{(i,j)}(t)+\Delta\tau_{(i,j)} \tag{8}$$

In this algorithm, when an ant moves to pixel (i, j), the pheromone left at pixel (i, j) is $G_{(i,j)}(x,y)/C$. Thus, the pheromone deposition is proportional to the gradient of that pixel. ρ denotes the evaporate coefficient.

(4) Termination rule.
The termination of this algorithm is achieved by a pre-defined number of cycles, for which each cycle contains a fixed

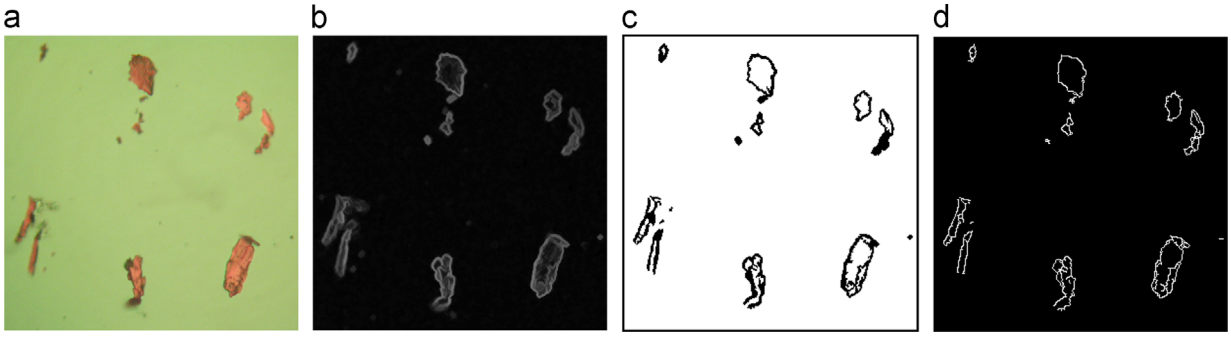

Fig. 2. The edge detection of the ferrograph images. (a) Original image, (b) morphological gradient image, (c) initial edges of wear particles, and (d) final edges of wear particles.

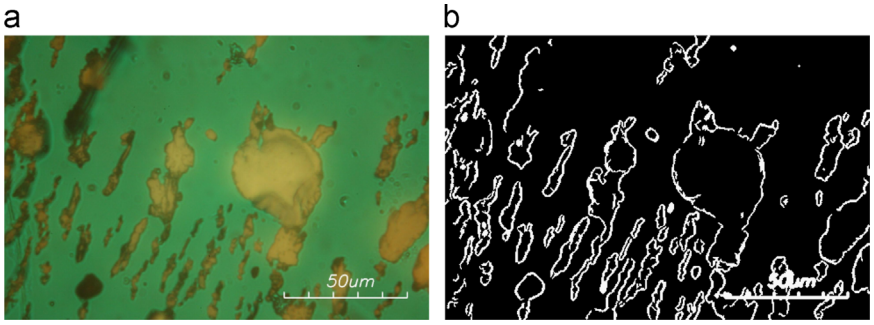

Fig. 3. The edge detection of wear particles. (a) Original image, and (b) IACO.

number of ants moving steps. The number of moving steps is related to the image size and the total number of ants. The number of iterations is selected to be 50, and the moving steps of each ant is chosen to be 300 for this algorithm.

Fig. 2(d) shows the final results of edge detection of wear particles.

3.4. Experimental results

Ferrograph images (600×400) taken from mining and petrochemical equipment are examined in this study. A number of experiments are employed to determine suitable algorithm parameters. In the proposed algorithm, the initial value for a pheromone is set to 0.01. The adjustment factors α and β influences the pheromone concentration and heuristic information respectively. Both α and β are set to 0.5 in this study. The pheromone evaporate coefficient ρ is set to 0.3. The memory length is set to 40.

Fig. 3(a) shows an original ferrograph image with wear particles of different sizes, shapes and degrees of brightness. Fig. 3 (b) shows the result of IACO. While it appears that IACO could extract most of the edges of the wear particles, this method also has limitations, such as false edges and unclosed edges, Furthermore, it misses some of the edge features. In addition, for images that have many particles, this method is time consuming because too many ants are needed to search the edges.

To obtain closed, single-pixel edges of wear particles, we propose another image segmentation method by combining the watershed algorithm and the ant colony algorithm.

4. Wear particle segmentation based on combined watershed and ant colony algorithm (CWACA)

The watershed algorithm, introduced initially by Vincent [35], is an image segmentation method based on region-generation strategy. Watershed transformation was simulated based on an immersion process. At the end of this immersion process, each minimum is completely surrounded by dams, which delimit its associated catchment basin. Compared with other algorithms, the watershed algorithm for image segmentation has certain advantages, such as high precision, high speed, and continuous edges, as well as disadvantages of over-segmentation due to its extreme sensitivity to noise in certain cases. Thus, the marker-watershed algorithm was later proposed to overcome over-segmentation. However, when the marker-watershed algorithm is applied to ferrograph image segmentation, because of the complex morphology and surface texture of wear particles, especially the large abnormal wear particles, over-segmentation is inevitable. To overcome the disadvantage of the watershed algorithm, the new image segmentation method, CWACA, is proposed in this study.

The main principle of CWACA is the following.

The marker-watershed algorithm is adopted to obtain the initial segmentation of wear particles. The improved ant colony clustering algorithm is later used to obtain the accurate segmentation of wear particles, especially the large abnormal wear particles.

The steps of wear particle segmentation based on CWACA are as follows.

4.1. Initial segmentation of wear particles

First, the marker-watershed algorithm is applied on the ferrograph gradient images to obtain an initial segmentation of wear particles.

$$SEG_w(x,y) = WS(G_{color}(x,y)), \tag{9}$$

where WS () is a watershed transformation and G_{color} (x, y) represents the color morphological gradient image.

Fig. 4(a) shows an original ferrograph image, and Fig. 4(b) shows the segmentation result of marker-watershed transformation. It is determined that the initial segmentation of wear particles could be obtained using the marker-watershed algorithm. However, due to the noise and uneven distributed gray level on particle surfaces, over-segmentation occurs on the surfaces of large wear particles, as shown

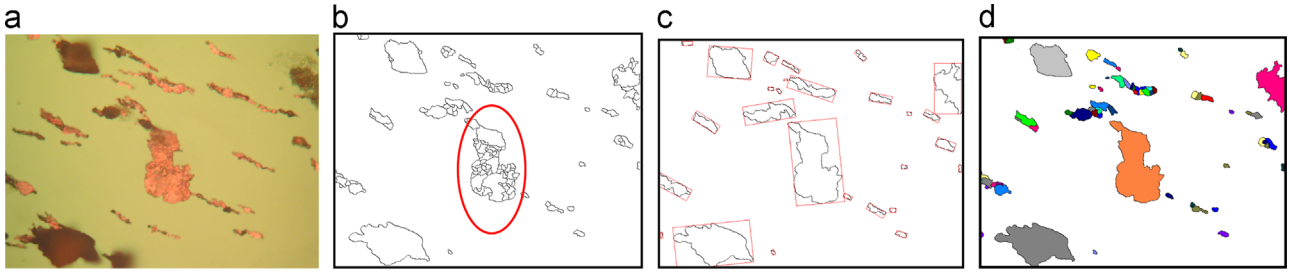

Fig. 4. CWACA process. (a) Original image, (b) watershed segmentation, (c) ant colony clustering, and (d) CWACA segmentation.

in the ellipse in Fig. 4(b). To solve the over-segmentation of large wear particles, the improved ant colony clustering algorithm is therefore applied in our study.

4.2. Improved ant colony clustering

In this study, the regions obtained from marker-watershed segmentation are considered as food for artificial ants. The improved ant colony clustering algorithm along with differences in color components and the dynamic radius is later used to search regions that have similar features. Thus, by merging the over-segmented regions, a better segmentation result of wear particles is obtained.

4.2.1. Cluster centroids

The $SEG_w(x, y)$ represents the segmented image after the watershed transformation. It consists of many regions $Z=\{Z_i|i=1, 2, 3,\ldots, n\}$, where n is the number of divided regions and the ith region $Z_i=\{p_{i1}, p_{i2},\ldots, p_{im}\}$ includes m pixels. Each region is considered as an ant, and C_i (x, y) represents the centroid of the ith region. Thus, C_i (x, y) is defined as

$$C_i(x,y)=\frac{\sum_{k=1}^{m} p_{ik}(x,y)}{m},\quad i=1,2,\cdots,n. \tag{10}$$

4.2.2. Dynamic clustering radius

The clustering radius is the distance that the ants search. The clustering radius in the traditional ACO algorithm is constant and does not reflect the changing results due to dynamic mergers of similar regions. Therefore, with the merger of different regions, the search radius should be adjusted accordingly.

The area A of each region is obtained by counting the number of pixels of each region. The equivalent radius r corresponding to each region is then calculated by

$$r=\sqrt{A/\pi}. \tag{11}$$

The dynamic clustering radius R is defined as

$$R=n\times r, \tag{12}$$

where n is a constant and $n=3$ in this study.

4.2.3. Setting of the pheromone

At moment t, the pheromones remaining on the path from region i to j is defined as

$$\tau_{ij}(t)=\begin{cases}1, & d_{ij}\le R\\ 0, & d_{ij}>R\end{cases}, \tag{13}$$

where d_{ij} is the Euclidean distance of the cluster centroids of region i and j.

4.2.4. Improved ant colony clustering criteria

The clustering probability of region i and j is determined by the following formula:

$$p_{ij}(t)=\begin{cases}\frac{\tau_{ij}^{\alpha}(t)\eta_{ij}^{\beta}(t)}{\sum_{s\in S}\tau_{sj}^{\alpha}(t)\eta_{sj}^{\beta}(t)}, & S=\{X_s|d_{sj}\le R, S=1,2,\cdots,N\}\\ 0, & \text{otherwise}\end{cases}, \tag{14}$$

where S is the set of all available regions that ant i can choose in one step.

The heuristic guide function is $\eta_{ij}(t)=1/d_{ij}$, which denotes the desired degree of clustering between region j and i. The guide function is inversely proportional to the distance between the two regions only without taking into account the color differences of the two regions. Therefore, in our algorithm, the color difference of the two regions is introduced into the guide function, and the improved guide function is defined as

$$\eta'_{ij}=\frac{R}{d_{ij}+\Delta C_{ij}}, \tag{15}$$

where R is the clustering radius, d_{ij} is the distance between two regions, ΔC_{ij} is the color difference between region i and j. Thus, it is defined as

$$\Delta C_{ij}=(\Delta a_{ij})^2+(\Delta b_{ij})^2 \tag{16}$$

where Δa_{ij} and Δb_{ij} denote the difference of two color components in the CIELAB color space of two regions, respectively.

If the clustering probability P_{ij} (t) of region i and j is greater than a pre-set threshold P_0, region i merges with region j.

4.3. Corrections of clustering

The accurate segmentation of large wear particles is realized by using the improved ant colony clustering algorithm. However, for wear particle chains that contain some tiny particles that may have similar features, incorrect merger may occur in some cases, as shown in Fig. 4(c). Therefore, the discrimination and correction of clustering is applied.

Wear particle chains may appear as elongated, and large abnormal wear particles tend to appear as layered, flaky or chunky. Therefore, shape parameter, which is the aspect ratio, can be used to distinguish large abnormal wear particles from wear particle chains.

Normally, except the cutting wear particles, the aspect ratio of large abnormal wear particles is small. Thus, in our algorithm, the aspect ratio threshold *fiber* is set to 2. Then, the aspect ratio of each region obtained from the ant colony clustering process is calculate. If the aspect ratio of a region is smaller than the pre-set threshold, the ant colony clustering result is considered to be the final result; otherwise, the ant colony clustering result is discarded, and the watershed segmentation result is retained.

Through the above process, the segmentation of abnormal wear particles can obtained, while at the same time, the incorrect

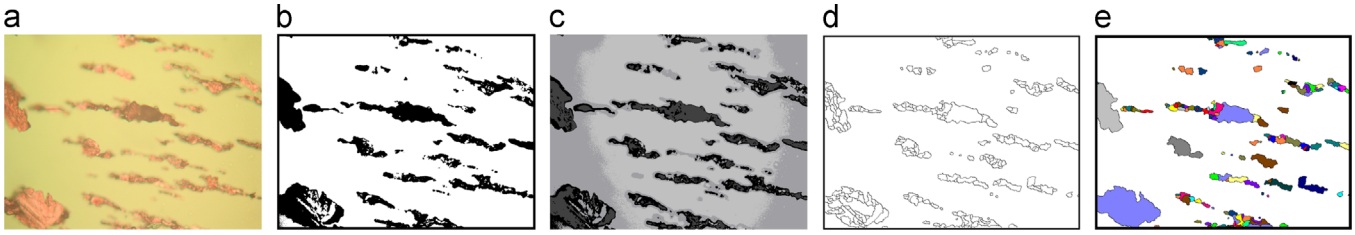

Fig. 5. Segmentation results of ferrograph image 1. (a) Original image, (b) K-means, (c) FCM, (d) marker-watershed, and (e) CWACA segmentation.

Fig. 6. Segmentation results of ferrograph image 2. (a) Original image, (b) K-means, (c) FCM, (d) marker-watershed, and (e) CWACA segmentation.

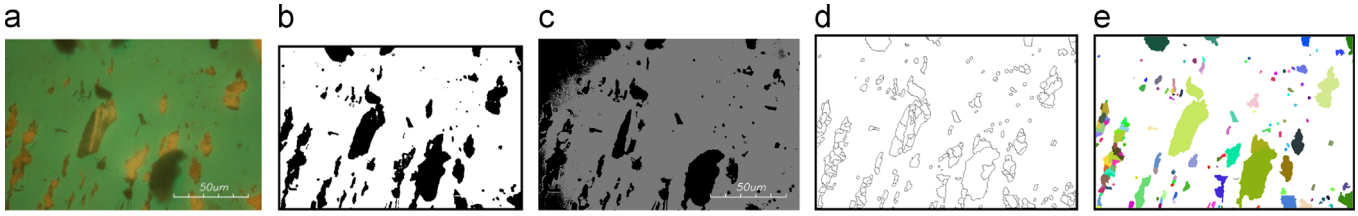

Fig. 7. Segmentation results of ferrograph image 3. (a) Original image, (b) K-means, (c) FCM, (d) marker-watershed, and (e) CWACA segmentation.

merger of tiny wear particles on deposited chains can be avoided. Fig. 4(d) is the final result of CWACA segmentation.

5. Experimental results

These experimental ferrograph images are taken from the petrochemical equipment. The image size is 800×600 pixels. The proposed algorithm, CWACA, is developed based on VC ++ 6.0 and OpenCV 1.0 platform. After a number of experiments, for the CWACA, the adjustment factor α and β are set to 0.5, the number of iterations is set to 30, and the clustering threshold is set to 0.1

Figs. 5–7 show the experimental segmentation results of ferrograph images using K-means clustering, fuzzy C-means (FCM) clustering, marker-watershed transformation and the proposed CWACA, respectively. In the result of the CWACA, the divided wear particles are presented with different colors.

When the K-means clustering method is used for image segmentation, it must specify the number of clusters K. If $K=2$, the separation between wear particles and image background could be initially realized. However, because of the uneven brightness of image background, in some cases, as shown in Fig. 6(b), part of the image background is likely to be segmented into wear particles. If $K>2$, because of the minimal color difference between some wear particles, it is difficult to achieve the exact accurate segmentation among wear particles.

While the fuzzy C-means (FCM) clustering is an unsupervised clustering method that can automatically calculate the number of clusters, when using this method for ferrograph image segmentation, due to the uneven brightness of image background and wear particles, it is also difficult to achieve the exact split between wear particles, as shown in Figs. 5–7(c).

Due to the immerse mechanism of watershed algorithm, the single-pixel-wide, connective, closed contours of wear particles can result when the marker-watershed algorithm is applied to the ferrograph images, and wear particles can be completely separated, even with wear particles having low contrast and weak boundaries. However, as evidenced from Figs. 5–7(d), certain wear particles, especially the large abnormal wear particles, are mistakenly separated into tiny particles.

Compared with the previous methods, the proposed method CWACA does not require a pre-set number of clusters. Furthermore, it is a hybrid method. It not only takes the advantages of watershed, such as simplicity, speed and complete division of the image but also takes the advantages of ant colony algorithm, such as intelligent search and heuristic clustering. As the results, each part of the ferrograph images are properly segmented into wear particles and background, tiny wear particles on deposited chains, and large abnormal wear particles, as shown in Figs. 5–7(e).

The above method has been tested with a large number of ferrograph images. The results have proven that it is effective to segment wear particles of different sizes, especially for large abnormal wear particles. For the tiny wear particles in deposited chains, the accuracy of the segmentation result needs to be improved, although it is not as important to condition monitoring and failure diagnosis as the large abnormal wear particles. Also, the computing efficiency needs to be improved when this method is used for the ferrograph image with a large quantity of wear particles.

6. Conclusions

Ferrography is a very useful means to determine the wear condition of machines. Wear particle segmentation is the critical

first step for intelligent ferrography based on computer image analysis.

Two segmentation methods of wear particles based on ant colony algorithm are proposed in this paper.

The first method uses the threshold algorithm to obtain initial edge points of wear particles. These points are then input into the modified ant colony algorithm, which utilizes the color of the pixel as the heuristic information. While the experimental results indicate that most of the edges of wear particles can be extracted using this method, it is time-consuming, and the appearance of false and unclosed edges limits this technique′s application.

The second method adopts marker-watershed to obtain a preliminary separation of wear particles. The improved ant colony clustering algorithm is later used to merge the over-segmented regions. During this process, not only the color feature but also the position feature of each region is taken as heuristic information, so that better segmentation results can be obtained. This method enables the segmentation of different types of wear particles, especially for the large abnormal wear particles and particle chains. Furthermore, this technique presents each wear particle with a closed single-pixel-width contour, which leads to the possibility for the following analysis of wear particles. These experiments demonstrated that this presented method could generate reasonable wear particle segmentation, thereby illustrating the method′s practical value.

Acknowledgments

This research is supported by the National Natural Science Foundation of China (No. 51205202) and by the Priority Academic Program Development of Jiangsu Higher Education Institutions (PAPD).

References

[1] B.J. Roylance, Ferrography—then and now, Tribol. Int. 38 (10) (2005) 857–862.
[2] N. Eliaz, R.M. Latanision, Preventative maintenance and failure analysis of aircraft components, Corros. Rev. 25 (1–2) (2007) 107–144.
[3] O. Levi, N. Eliaz, Failure analysis and condition monitoring of an open-loop oil system using ferrography, Tribol. Lett. 36 (1) (2009) 17–29.
[4] G.W. Stachowiak, P. Podsiadlo, Towards the development of an automated wear particle classification system, Tribol. Int. 39 (12) (2006) 1615–1623.
[5] S. Raadnui, Wear particle analysis–utilization of quantitative computer image analysis: a review, Tribol. Int. 38 (10) (2005) 871–878.
[6] M.S. Laghari, Q.A. Memon, G.A. Khuwaja, Knowledge based wear particle analysis, Int. J. Inf. Technol. 1 (3) (2004) 91–95.
[7] G.P. Stachowiak, G.W. Stachowiak, P. Podsiadlo, Automated classification of wear particles based on their surface texture and shape features, Tribol. Int. 41 (1) (2008) 34–43.
[8] X.P. Yan, C.H. Zhao, Z.Y. Lu, et al., A study of information technology used in oil monitoring, Tribol. Int. 38 (10) (2005) 879–886.
[9] N.K. Myshkin, H. Kong, A.Y. Grigoriev, et al., The use of color in wear debris analysis, Wear 251 (2001) 1218–1226.
[10] Z. Peng, T.B. Kirk, Wear particle classification in a fuzzy grey system, Wear 225–229 (1999) 1238–1247.
[11] U. Cho, J.A. Tichy, Quantitative correlation of wear debris morphology grouping and classification, Tribol. Int. 33 (2000) 461–467.
[12] V.D. Gonçalves, L.F. Almeida, M.H. Mathias, Wear particle classifier system based on an artificial neural network, J. Mech. Eng. 56 (2010) 284–289.
[13] T.P. Sperring, T.J. Nowel, SYCLOPS–a qualitative debris classification system developed for RAF early failure detection centres, Tribol. Int. 38 (10) (2005) 898–903.
[14] Z. Peng, S. Goodwin, Wear-debris analysis in expert systems, Tribol. Lett. 11 (3–4) (2001) 177–184.
[15] J. Wang, X. Wang, A wear particle identification method by combining principal component analysis and grey relational analysis, Wear 304 (1–2) (2013) 96–102.
[16] T.H. Wu, J.Q. Wang, J.Y. Wu, et al., Wear characterization by an on-line ferrograph image, Proc. IMechE Part J: J. Eng. Tribol. 225 (2011) 23–34.
[17] S.Q. Yu, X.J. Dai, Wear particle image segmentation method based on the recognition of background color, Tribology 27 (5) (2007) 467–471.
[18] G.M. Chen, Y.B. Xie, L.Z. Jiang, Application study of color feature extraction on ferrographic image classifying and particle recognition, China Mech. Eng. 17 (15) (2006) 1576–1579.
[19] J. Wang, L. Zhang, X. Wang, Combining k-means clustering and watershed algorithm for the segmentation of color ferrograph image, J. China Univ. Minning Technol. 42 (5) (2013) 866–872.
[20] F. Li, C. Xu, G.Q. Ren, J.W. Gao, Image segmentation of ferrography wear particles based on mathematical morphology, J. Nanjing Univ. Sci. Technol. 29 (1) (2005) 70–72.
[21] X. Hu, P. Huang, S. Zheng, On the pretreatment process for the object extraction in color image of wear debris, Int. J. Imaging Syst. Technol. 17 (5) (2007) 277–284.
[22] Y.J. Zhang, A survey of evaluation methods for image segmentation, Pattern Recognit. 29 (8) (1996) 1335–1346.
[23] M. Dorigo, V. Maniezzo, A. Colorni, Ant system: Optimization by a colony of cooperating agents, Trans. Syst., Man Cybern. Part B 26 (1) (1996) 29–41.
[24] O.A.M. Jafar, R. Sivakumar, Ant-based clustering algorithms A brief survey, Int. J. Comput. Theory Eng. 2 (5) (2010) 787–796.
[25] S.A. Etemad, T. White, An ant-inspired algorithm for detection of image edge features, Appl. Soft Comput. 11 (8) (2011) 4883–4893.
[26] Y. Tyagi, T.A. Puntambekar, P. Sexena, et al., A hybrid approach to edge detection using ant colony optimization and fuzzy logic, Int. J. Hybrid Inf. Technol. 5 (1) (2012) 37–46.
[27] H. Nezamabadi-pour, S. Saryazdi, E. Rashedi, Edge detection using ant algorithms, Soft Comput. 10 (7) (2006) 623–628.
[28] D. Lu, C. Chen, Edge detection improvement by ant colony optimization, Pattern Recognit. Lett. 29 (4) (2008) 416–425.
[29] J. Tian, W. Yu, L. Chen, et al., Image edge detection using variation-adaptive ant colony Optimization, Trans. Comput. Collect. Intell. V Lect. Notes Comput. Sci. 6910 (2011) 27–40.
[30] P.S. Shelokar, V.K. Jayaraman, B.D. Kulkarni, An ant colony approach for clustering, Anal. Chim. Acta. 509 (2) (2004) 187–195.
[31] W. Yang, L. Guo, T. Zhao, et al., Image segmentation method based on watersheds and ant colony clustering, Chin. J. Quantum Electron. 25 (1) (2008) 19–24.
[32] Y. Han, P. Shi, An improved ant colony algorithm for fuzzy clustering in image segmentation, Neurocomputing 70 (2007) 665–671.
[33] Z. Yu, O.C. Au, R. Zou, et al., An adaptive unsupervised approach toward pixel clustering and color image segmentation, Pattern Recognit. 43 (5) (2010) 1889–1906.
[34] A. Doğan, U. Aybars, Extraction of flower regions in color images using ant colony optimization, Procedia Comput. Sci. 3 (2011) 530–536.
[35] L. Vincent, P. Solille, Watershed in digital spaces: an efficient algorithm based immersion simulations, IEEE. Trans. Pattern Anal. Mach. Intell. 13 (6) (1991) 583–598.